AD-A066 179 NAVAL RESEARCH LAB WASHINGTON D C F/G 20/7
RADIAL EXPANSION OF A SELF-PINCHED BEAM WITH DISTRIBUTED ENERGY--ETC(U)
JAN 79 M I HAFTEL, M LAMPE, J B AVILES
UNCLASSIFIED NRL-MR-3908 SBIE-AD-E000 266 NL

1 OF 1
ADA
066179

END
DATE
FILMED
5-79
DDC

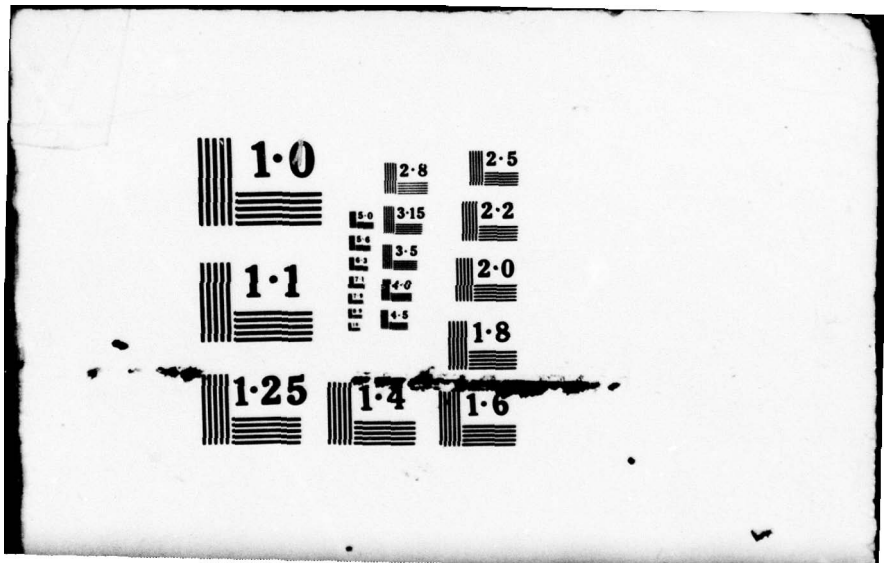
1·0
1·1
1·25
2·8
3·15
3·5
4·0
4·5
2·5
2·2
2·0
1·8
1·4
1·6

NRL Memorandum Report 3908

Radial Expansion of a Self-Pinched Beam with Distributed Energy

M. I. HAFTEL

Radiation-Matter Interaction Branch
Radiation Technology Division

MARTIN LAMPE

Plasma Theory Branch
Plasma Physics Division

and

J. B. AVILES

Radiation-Matter Interaction Branch
Radiation Technology Division

January 17, 1979

Work sponsored by the Naval Surface Weapons Center under subtask N60921-78-WR-W0023, Charged Particle Beam Theory

NAVAL RESEARCH LABORATORY
Washington, D.C.

SECURITY CLASSIFICATION OF THIS PAGE (When Data Entered)

REPORT DOCUMENTATION PAGE

READ INSTRUCTIONS BEFORE COMPLETING FORM

1. REPORT NUMBER (14) NRL-MR-
NRL Memorandum Report 3908

2. GOVT ACCESSION NO.

3. RECIPIENT'S CATALOG NUMBER (9)

4. TITLE (and Subtitle) (6)
RADIAL EXPANSION OF A SELF-PINCHED BEAM WITH DISTRIBUTED ENERGY•

5. TYPE OF REPORT & PERIOD COVERED
Interim report on a continuing NRL problem.

6. PERFORMING ORG. REPORT NUMBER

7. AUTHOR(s) (10)
Michael I. Haftel, Martin Lampe, Joseph B. Aviles

8. CONTRACT OR GRANT NUMBER(s)

9. PERFORMING ORGANIZATION NAME AND ADDRESS
Naval Research Laboratory
Washington, D.C. 20375

10. PROGRAM ELEMENT, PROJECT, TASK AREA & WORK UNIT NUMBERS
NRL Problem R08-93B

11. CONTROLLING OFFICE NAME AND ADDRESS (11) 17
Naval Surface Weapons Center
White Oak, Silver Spring, Maryland 20910

12. REPORT DATE
January 1979

13. NUMBER OF PAGES
54

14. MONITORING AGENCY NAME & ADDRESS(if different from Controlling Office) (12) 56p. (16) F32391 (17) RF32391801

15. SECURITY CLASS. (of this report)
UNCLASSIFIED

15a. DECLASSIFICATION/DOWNGRADING SCHEDULE

16. DISTRIBUTION STATEMENT (of this Report)
Approved for public release; distribution unlimited.
(18) SBIE

DDC RECEIVED MAR 22 1979 B

17. DISTRIBUTION STATEMENT (of the abstract entered in Block 20, if different from Report)
(19) AD-E000 266

18. SUPPLEMENTARY NOTES
This research was sponsored by the Naval Surface Weapons Center under Subtask N60921-78-WR-W0023.

19. KEY WORDS (Continue on reverse side if necessary and identify by block number)
Relativistic beams
Electron beams
Beam propagation
Straggled electron beam
Self-pinched beams

20. ABSTRACT (Continue on reverse side if necessary and identify by block number)
The structure and radial expansion of a relativistic particle beam are calculated, in the presence of Coulomb scattering. The beam is assumed to be self-pinched and paraxial, but to have a distribution in energy. For the case in which the beam energy spread is small enough to satisfy $(\beta\gamma)_{min}\,\overline{\beta^{-1}\gamma^{-1}} > 1/2$, the entire beam expands self-similarly at an exponential rate proportional to $\overline{\beta^{-1}\gamma^{-1}}$, where $\beta \equiv v/c$, $\gamma^{-2} \equiv 1 - \beta^2$, and bar denotes average over γ. The beam profile is calculated.
(Continues)

DD FORM 1 JAN 73 1473 EDITION OF 1 NOV 65 IS OBSOLETE
S/N 0102-014-6601

251950

20. Abstract (Continued)

exactly in this case. If the inequality is not satisfied, low-γ particles expand faster than the main beam, at an exponential rate proportional to $(2\beta\gamma)^{-1}$. Approximate time-dependent solutions, including initial transients, are presented for both cases.

CONTENTS

RADIAL EXPANSION OF A SELF-PINCHED BEAM WITH DISTRIBUTED ENERGY

I. Introduction

An electron or ion beam can propagate through a gaseous medium in a self-pinched mode, provided that the conductivity of the medium is high enough to neutralize the beam space charge, but not so high as to completely neutralize the beam current. If scattering and energy loss are neglected, the beam propagates in a static equilibrium, with its transverse kinetic pressure just balancing the magnetic pinch force. This condition is equivalent to the statement that the mean transverse beam temperature $\bar{T}$, i.e. the transverse random kinetic energy per particle, averaged over all beam particles, takes on the Bennett value[1,2]

$$\bar{T} = \frac{q \langle \bar{v}_z \rangle \mu_o I_o}{8\pi} , \tag{1.1}$$

where q is the beam particle charge, $\langle \bar{v}_z \rangle$ the mean axial velocity, and I_o the net current (beam current less return current).

When weak multiple Coulomb scattering by the medium is taken into account, the beam propagates in a quasi-static equilibrium. As scattering adds to the transverse random kinetic energy, the beam expands adiabatically, so as to maintain the pressure balance condition (1.1). In the case of a paraxial, monoenergetic beam, with axial

Note: Manuscript submitted November 9, 1978.

velocity βc and particle energy $mc^2\gamma$, Eq. (1.1) becomes

$$T = T_B \equiv \frac{q\beta c\, \mu_o I_o}{8\pi} , \tag{1.2}$$

and it has been shown that the beam density $Nn(r,t)$ takes on a Bennett profile[3]

$$n(r,t) = \frac{1}{\pi a^2} \frac{1}{[1 + r^2/a^2(t)]^2} , \tag{1.3}$$

and the Bennett radius $a(t)$ expands in accordance with the Nordsieck equation[3-5],

$$\frac{d}{dt} [\ell n\, a^2(t)] = \frac{\epsilon_\gamma}{T_B} , \tag{1.4}$$

where ϵ_γ is the rate of increase of transverse kinetic energy per particle, due to scattering.

An actual propagating beam may be far from monoenergetic, due either to initial energy spread produced in accelerating and injecting the beam, or to energy spread resulting from propagation. The purpose of this paper is to investigate the structure and expansion rate of a beam with a distribution of particle energies. The interesting effects arise mainly from the dependence of the Coulomb scattering index ϵ_γ on energy (i.e. on γ). For an ultra-relativistic electron beam with $\gamma \geq 100$, ϵ_γ is given approximately by[6]

$$\epsilon_\gamma = \frac{8\pi\, n_s\, Z(Z+1)q^2e^2}{(4\pi\epsilon_o)^2\, mc\beta\gamma} \ell n\, (210\, Z^{-1/3}), \tag{1.5a}$$

where n_s and Ze are the density and charge of scattering nuclei. For ions or lower energy electrons[4,6], $\ell n\, (210\, Z^{-1/3})$ is replaced by

$\frac{1}{2}$ ℓn ($\hbar$ $Z^{1/3}/mc\beta\gamma a_o$), i.e.

$$\epsilon_\gamma = \frac{4\pi n_s Z(Z+1)q^2e^2}{(4\pi\epsilon_o)^2 mc\beta\gamma} \ell n (\hbar Z^{1/3}/mc\beta\gamma a_o) \qquad (1.5b)$$

where a_o is the Bohr radius. In any event, $\epsilon_\gamma \propto \gamma^{-1}$ for relativistic particles (neglecting both the deviation of β from unity and the possible weak logarithmic dependence on γ). Thus one expects low energy particles to spread to the outside of the pinched beam and expand more rapidly. It is by no means obvious a priori how to average over γ to arrive at a mean expansion rate for the beam as a whole, or even if such a rate is well defined.

In the rest of this introduction, we shall summarize the main assumptions and results of the paper. Our assumptions are similar to those of previous treatments[3-5], viz:

(i) Paraxial beam, i.e. transverse velocities small compared to the axial velocity βc. In conventional relativistic beam terminology, this means low net $\upsilon/\gamma \equiv I_o(1.7 \times 10^4 \beta\gamma$ amsp), where I_o is the net current characterizing the pinch force.

(ii) Azimuthal symmetry.

(iii) No external magnetic field.

(iv) Beam subject to small-angle multiple elastic scattering by the medium, but collisions between beam particles are neglected (usually a very well satisfied assumption). Thus there is no reason to expect different energy components of the beam to be in overall thermodynamic equilibrium at a common temperature.

(v) An initial energy spread is assumed, but the energy of any particular beam particle is assumed constant in time. Most of our results can easily be modified to include deterministic energy

losses, e.g. due to multiple inelastic Coulomb collisions, or to self-generated inductive electric fields that drive return currents in the resistive medium (known as Ohmic losses). In an ultra-relativistic electron beam ($\gamma \geq 100$), bremsstrahlung emission becomes a dominant energy loss process, and also leads to a rapid spreading of the energy distribution, which is called "straggling". The mathematical complexities of treating straggling self-consistently with radial beam expansion are not addressed in this paper, but qualitative insights into this self-consistent problem can be obtained by using an initial energy distribution that is appropriate for a straggled beam.

(vi) Uniform fractional neutralization of beam space charge and current, i.e. if $J_b(r,t)\beta c$ and $J_b(r,t)$ are the beam charge and current density, then it is assumed that a charge density - $\alpha_E J_b(r,t)/\beta c$ and a current density - $\alpha_M J_b(r,t)$ occur in the medium, where α_E and α_M are constants. Typically charge neutralization is complete, $\alpha_E = 1$ (except at the beam head in a neutral gas), while current neutralization is partial, $0 \leq \alpha_M < 1$.

(vii) Quasi-static beam equilibrium, i.e. radial beam expansion slow compared to individual particle oscillations in the pinch field.

(viii) Isotropic and isothermal velocity distributions, for beam particles with a particular value of γ, are assumed in deriving fluid equations from the Boltzmann equation.

Our principal results are as follows. In Sec. IIA we derive a set of fluid equations for the beam, and in Sec. IIB we find an exact solution of these equations, provided that the beam energy spread is

small enough to satisfy

$$\bar{\epsilon}/\epsilon_\gamma < 2, \tag{1.6a}$$

i.e. approximately,

$$\gamma\,\overline{\gamma^{-1}} > \tfrac{1}{2} \tag{1.6b}$$

for all beam particles, where a bar indicates average over γ. In this case, the radial profile of particles with energy γ takes the form

$$n_\gamma(r,t) = (N_\gamma/\pi a_\gamma^2)[G(r/a(t))]^{\bar{\epsilon}/\epsilon_\gamma} \tag{1.7a}$$

$$\approx (N_\gamma/\pi a_\gamma^2)[G(r/a(t))]^{\gamma\,\overline{\gamma^{-1}}}\,, \tag{1.7b}$$

where $a(t)$ is a characteristic radius for the whole beam, $G(r/a(t))$ is a γ-independent function with $G(0) = 1$, the $a_\gamma(t)$ are characteristic radii for different values of γ, defined by

$$\pi a_\gamma^{\,2}(t) n_\gamma(0,t) \equiv \int dr 2\pi r n_\gamma(r,t) \equiv N_\gamma\,, \tag{1.8}$$

and N_γ is the distribution over γ, normalized to unity. The ratio $a_\gamma(t)/a_{\gamma'}(t)$ is time-independent, for any values of γ and γ', and all of the a_γ, as well as a, expand as

$$\frac{d}{dt}\,\ell n\, a^2 = \frac{\bar{\epsilon}}{T_B}\,, \tag{1.9}$$

with T_B given by Eq. (1.2). The beam thus expands in a completely self-similar fashion. Numerical solutions for the function $G(r/a)$ are found; if the condition (1.6) is well satisfied, G is close to the Bennett distribution.

In Sec. IIC, exact solutions of the Boltzmann equation are found for high γ particles, which are localized near the beam axis, where the pinch force is harmonic. The harmonic form of the pinch force implies that $n_\gamma(r)$ is Gaussian.

In Sec. IIIA a different approach is used to derive envelope equations for the a_γ from the single particle equations of motion. In Sec. IIIB, these equations are used to show that low-γ particles which violate Eq. (1.6) (typically such particles would constitute a low-amplitude tail of the energy distribution N_γ at low γ) expand, asymptotically in time, at an exponential rate faster than that of the beam as a whole,

$$\frac{d}{dt} \ell n\, a_\gamma^2(t) = \frac{\epsilon_\gamma}{2T_B} . \tag{1.10}$$

Thus, given enough time, these particles "evaporate" from the beam, leaving behind a reduced-current beam that expands completely self-similarly (if no further straggling occurs).

In Sec. IV, we derive approximate models that specify the time dependence of the $a_\gamma(t)$, given any initial conditions. We examine the approach to the completely self-similar solution if (1.6) is satisfied, as well as the approach to the asymptotic solution (1.10) for particles that violate (1.6). Numerical solutions are given for some particular cases. We find that the approach to the time-asymptotic state takes a time that is typically several times the characteristic time scale $T_B/\bar{\epsilon}$. Thus transient effects can be important. Equation (1.9) is found to be reasonably accurate, even during the transient period.

II. Kinetic and Hydrodynamic Treatment

A. Fundamental Equations

We begin our discussion in this section with the Boltzmann equation for the transverse dynamics of a self-pinched beam propagating in a gas,

$$\frac{\partial f_\gamma}{\partial t} + v_r \frac{\partial f_\gamma}{\partial r} - r\omega_\beta^2 \frac{\partial f_r}{\partial v_r} = \frac{\epsilon_\gamma}{m\gamma} \frac{\partial^2 f_\gamma}{\partial v^2} \tag{2.1}$$

where $f_\gamma(r,\underset{\sim}{v},t)$ is the beam distribution over radial position r, transverse velocity $\underset{\sim}{v}$, and relativistic energy $mc^2\gamma$. Azimuthal symmetry is assumed throughout. The right hand side of (2.1) has the form of a velocity space diffusion, due to the effect of multiple small-angle Coulomb scattering of beam particles off gas atoms, with the quantity ϵ_γ given by Eq. (1.5). The distribution $f_\gamma(r,\underset{\sim}{v},t)$ is normalized so that

$$n_\gamma(r,t) = \int d^2\underset{\sim}{v} f_\gamma(r,\underset{\sim}{v},t) \tag{2.2}$$

is the spatial distribution of beam particles with energy $mc^2\gamma$ (per unit γ),

$$N_\gamma = \int_0^\infty dr 2\pi r n_\gamma(r,t) \tag{2.3}$$

is the distribution of beam particles over γ, assumed in this paper to be time independent, and

$$\int d\gamma N_\gamma = 1. \tag{2.4}$$

We also define a spatial distribution for the whole beam

$$n(r,t) \equiv \int_o^\infty d\gamma n_\gamma(r,t). \tag{2.5}$$

The magnetic self-pinch force (as well as any electrostatic force due to unneutralized beam space charge) is characterized by the betatron frequency $\omega_\beta(r,t)$, defined by

$$\omega_\beta^2(r,t) = \frac{q\beta c\mu_o I(r,t)}{2\pi m\gamma r^2}, \tag{2.6}$$

where $I(r,t)$ is the effective net current flowing within radius r, defined by

$$\begin{aligned} I(r,t) &= [(1 - \alpha_M) - \beta^{-2}(1 - \alpha_E)] I_b(r,t), \\ &\equiv (1 - \alpha) I_b(r,t) \end{aligned} \tag{2.7}$$

where

$$I_b(r,t) \equiv I_b(\infty,t) \int_o^r dr 2\pi r n(r,t) \tag{2.8}$$

is the beam current within radius r, and we define also

$$I_o \equiv I(r \to \infty, t). \tag{2.9}$$

Since collisions between beam particles are neglected, different γ components of the beam will not come into mutual thermal equilibrium; these different components are, however, coupled through the nonlinear term in (2.1) involving the pinch ω_β^2.

By taking velocity moments of Eq. (2.1) (and assuming isotropy), we arrive at the hydrodynamic equations,

$$\frac{\partial n_\gamma}{\partial t} + \frac{1}{r}\frac{\partial}{\partial r}(r n_\gamma V_\gamma) = 0, \tag{2.10}$$

$$m\gamma\, N n_\gamma \left(\frac{\partial V_\gamma}{\partial t} + V_\gamma \frac{\partial V_\gamma}{\partial r}\right) = -\, m\gamma\, \omega_\beta^{\,2} r N n_\gamma - \frac{\partial P_\gamma}{\partial r}\,, \tag{2.11}$$

$$\frac{\partial P_\gamma}{\partial r} + \frac{1}{r}\frac{\partial}{\partial r}(r P_\gamma V_\gamma) + \frac{P_\gamma}{r}\frac{\partial}{\partial r}(r V_\gamma) + \frac{1}{r}\frac{\partial}{\partial r}(r Q_\gamma) = \epsilon_\gamma N n_\gamma, \tag{2.12}$$

where V_γ, P_γ and $\underset{\sim}{Q}_\gamma$ are the flow velocity, pressure, and heat flow for particles with a given γ, defined by

$$\underset{\sim}{V}_\gamma(r,t) \equiv \int d^2\, \underset{\sim}{v}\, \underset{\sim}{v}\, f_\gamma(r,\underset{\sim}{v},t)/n_\gamma(r,t) \tag{2.13a}$$

$$P_\gamma(r,t) \equiv \int d^2\, \underset{\sim}{v}\, \tfrac{1}{2}\, m\gamma\, [\underset{\sim}{v} - V(r,t)]^2 N f_\gamma(r,\underset{\sim}{v},t) \tag{2.13b}$$

$$Q_\gamma(r,t) \equiv \int d^2\, \underset{\sim}{v}\, \tfrac{1}{2}\, m\gamma\, (\underset{\sim}{v} - \underset{\sim}{V})^2 (\underset{\sim}{v} - \underset{\sim}{V}) N f_\gamma(r,\underset{\sim}{v},t). \tag{2.13c}$$

N is the total number of beam particles per unit length, and we also define a temperature $T_\gamma(r,t)$ by

$$N T_\gamma(r,t) = P_\gamma(r,t)/n_\gamma(r,t) \tag{2.13d}$$

Following previous treatments of beam expansion[3], we assume that $T_\gamma(r,t) = T_\gamma(t)$ is spatially uniform (i.e. the beam particles with any given γ are isothermal), and look for similarity solutions of the form

$$n_\gamma(r,t) = \frac{1}{\pi a_\gamma^{\,2}}\, \bar{n}_\gamma \left(\frac{r}{a_\gamma(t)}\right) \tag{2.15}$$

It follows from Eqs. (2.10) and (2.15) that the radial expansion is uniform, i.e.

$$V_\gamma(r,t) = \frac{\dot{a}_\gamma(t)}{a_\gamma(t)}\ r,$$

and Eqs. (2.11) and (2.12) reduce to the following form:

$$\dot{T}_\gamma(t)\ \frac{\partial}{\partial r}\ n_\gamma(r,t) + m\gamma\omega_\beta^{\,2}(r,t)rn_\gamma(r,t) = -m\gamma n_\gamma(r,t)r\ \frac{\ddot{a}_\gamma(t)}{a_\gamma(t)}\ , \quad (2.16)$$

$$\dot{T}_\gamma(t) + 2T_\gamma(t)\ \frac{\dot{a}_\gamma(t)}{a_\gamma(t)} - \epsilon_\gamma = 0. \quad (2.17)$$

We consider only the case of quasi-static equilibrium, in which ω_β^{-1} is short compared to the scattering time scale T_γ/ϵ_γ, flow velocities are small compared to internal velocities, and the right hand side of Eq. (2.16) can be neglected.* The hydrodynamic equations then reduce to

$$T_\gamma(t)\ \frac{\partial}{\partial r}\ n_\gamma(r,t) + m\gamma\omega_\beta^{\,2}(r,t)r\ n_\gamma(r,t) = 0, \quad (2.18)$$

$$\dot{T}_\gamma(t) + 2T_\gamma(t)\ \frac{\dot{a}_\gamma(t)}{a_\gamma(t)} - \epsilon_\gamma = 0, \quad (2.19)$$

with $\omega_\beta^{\,2}(r,t)$ coupled to the n_γ through Eq. (2.6), and subject to the boundary condition (2.3). Equation (2.18) is simply transverse pressure balance, while Eq. (2.19) is the adiabatic expansion law, with the second term being PdV work and the third term the rate of

* Two comments are appropriate here. For r far outside the main beam, $\omega_\beta \to 0$, and for those few electrons that scatter out to this region, the dynamics is dominated by scattering rather than by the pinch force. Also, in dropping the right hand side of (2.16), we are also neglecting radial oscillations of a_γ (sausage mode) which occur if the beam is injected out of dynamic equilibrium.

energy input to the transverse plane, due to scattering.

Equations (2.18) and (2.19) have been solved in closed form for the special case of a monoenergetic beam[3], with the result

$$T = T_B \equiv \frac{q\beta c\, \mu_o I_o}{8\pi}, \tag{2.20}$$

$$n(r,t) = \frac{1}{\pi a^2(t)} \left(1 + \frac{r^2}{a^2(t)}\right)^{-2}, \tag{2.21}$$

$$\frac{d}{dt} \ell n\, a^2 = \frac{\epsilon_\gamma}{T_B} t. \tag{2.22}$$

Equation (2.20) is the well known Bennett pinch condition[1,2], Eq. (2.21) is the Bennett profile, while (2.22) is the Nordsieck equation. This simple solution (2.21), (2.22) is possible in the monoenergetic case only because the problem is not complicated by the coupling of different values of γ. In the general case, it can still be shown[2] directly from the hydrodynamic equations (2.18) and (2.19) that the Bennett condition holds for an averaged $\bar{T}$,

$$\bar{T} \equiv \int d\gamma N_\gamma T_\gamma(t) = T_B, \tag{2.23}$$

but there is no simple, general way to calculate the temperature T_γ of the separate γ components, i.e. the total internal energy is fixed by pressure balance with the magnetic pinch force, but energy can be apportioned among the various γ components in a way that depends on the detailed evolution.

B. Completely Self-Similar Expansion

In this section, we demonstrate that, provided the energy distribution N_γ satisfies a condition that will be specified, Eqs.

(2.18) and (2.19) have solutions that correspond to completely self-similar beam expansion, i.e. the profiles $n_\gamma(r,t)$ take the form

$$n_\gamma(r,t) = n_\gamma(r/a(t)), \tag{2.24}$$

where a is a γ-independent radius that characterizes the beam as a whole, and the temperatures T_γ remain constant,

$$\dot{T}_\gamma = 0. \tag{2.25}$$

Equation (2.19) then reduces to

$$T_\gamma \frac{d}{dt} \ell n\, a^2 = \epsilon_\gamma, \tag{2.26}$$

and to satisfy Eq. (2.23),

$$T_\gamma = T_B \epsilon_\gamma / \bar{\epsilon}\ . \tag{2.27}$$

Equation (2.26) can thus be rewritten as

$$\frac{d}{dt} \ell n\, a^2 = \frac{\bar{\epsilon}}{T_B}\ ; \tag{2.28}$$

where T_B is the Bennett relation, Eq. (1.2), and $\bar{\epsilon}$ is the average over γ of ϵ_γ, given by Eq. (1.5). Equation (2.28) is a generalized Nordsieck equation that follows exactly from the hydrodynamic equations (2.18) and (2.19) and the assumptions (2.24) and (2.25).

To solve for the density profiles $n_\gamma(r/a)$, we first rewrite Eq. (2.18) in the form

$$\frac{T_\gamma\ x\ dn_\gamma}{n_\gamma(x)dx} = -\ m\gamma r^2 \omega_\beta^2(x) = -4T_B \frac{I(r)}{I_o}\ , \tag{2.29}$$

where x is the dimensionless variable r/a, and we make use of Eqs. (2.6) and (1.2). We note that the right hand side of (2.29) is independent of γ. Therefore it must be possible to define a function G(x) such that

$$\frac{\bar{T}}{G}\frac{dG}{dx} = \frac{T_\gamma}{n_\gamma}\frac{dn_\gamma}{dx} . \tag{2.30}$$

We immediately obtain the universal form

$$n_\gamma(x) = C_\gamma[G(x)]^{\bar{T}/T_\gamma} = C_\gamma[G(x)]^{\bar{\epsilon}/\epsilon_\gamma} . \tag{2.31}$$

Since Eq. (2.30) only specifies G to within a multiplicative constant, we choose to require

$$G(0) = 1; \tag{2.32}$$

Eq. (2.31) may then be rewritten as

$$n_\gamma(x) = \frac{N_\gamma}{\pi a_\gamma^2}[G(x)]^{\bar{\epsilon}/\epsilon_\gamma} . \tag{2.33}$$

Next we rewrite Eqs. (2.29) and (2.30) in the form

$$\frac{x}{G}\frac{dG}{dx} = -4\frac{I(x)}{I_o} , \tag{2.34}$$

and write a differential form connecting I(x) to G(x),

$$\frac{1}{x}\frac{d}{dx}\frac{I(x)}{I_o} = 2\pi a^2 \int d\gamma n_\gamma(x) = 2\frac{a^2}{a_\gamma^2}\int d\gamma N_\gamma[G(x)]^{\bar{\epsilon}/\epsilon_\gamma} . \tag{2.35}$$

Integrating (2.33) over x yields an equation for the a_γ,

$$\frac{a_\gamma^2}{a^2} = 2\int_0^\infty dx\, x\,[G(x)]^{\bar{\epsilon}/\epsilon_\gamma} . \tag{2.36}$$

The coupled equations (3.34) - (3.36), with the boundary conditions (3.32) and

$$G'(0) = 0 \tag{2.37}$$

[which is equivalent to $I(x) \propto x^2$ for $x \to 0$], specify G and the a_γ (up to a scale factor in the radius), given any energy distribution N_γ. For a monotonic energy distribution, $N_\gamma = N\delta(\gamma - 1/\overline{\gamma^{-1}})$, the Bennett profile is a solution of these equations; in more general cases, numerical solution is required. Before presenting some numerical solutions, we discuss some general properties of the solutions.

The procedure just described is self-consistent if it is possible to normalize the resulting $n_\gamma(r)$, i.e. to satisfy Eq. (2.36). This requires that $[G(x)]^{\bar{\epsilon}/\epsilon_\gamma} \to 0$ faster than x^{-2}, for large x. Now according to Eq. (2.34),

$$G(x) \propto x^{-4}, \text{ for } x \to \infty, \tag{2.42}$$

and thus the results are self-consistent if

$$\bar{\epsilon}/\epsilon_\gamma \approx \overline{\gamma^{-1}} \quad \gamma > \tfrac{1}{2} \tag{2.43}$$

for all γ. If (2.43) is not satisfied, there is no completely self-similar solution, i.e. the conditions (2.24) and (2.25) cannot be imposed.

Equation (2.33) in itself gives considerable insight into the nature of the solution, and what happens when the assumption of completely self-similar expansion breaks down. Consider first the case $\gamma \langle \gamma^{-1} \rangle \gg 1$. For $r \ll a$, G must have the form

$$G(r/a) \approx 1 - r^2/r_o^2, \tag{2.44}$$

and thus

$$n_\gamma(r) \approx r_o^{-2} \exp\left(- \frac{r^2}{r_o^2} \gamma \overline{\gamma^{-1}} \right) \tag{2.45}$$

for $\gamma \langle \gamma^{-1} \rangle \gg 1$. Thus high γ particles are tightly confined near the beam axis, in a Gaussian profile, whose width a_γ scales as $\gamma^{-1/2}$. For $\gamma \overline{\gamma^{-1}} = 1$,

$$n_\gamma(r) = (N_\gamma/\pi a_\gamma^2) G(r/a) \tag{2.46}$$

falls off as r^{-4} at large r, like the Bennett profile; in fact the numerical solutions indicate that G is close to the Bennett profile, if the condition (2.43) for the existence of a completely self-similar solution is well satisfied. For $\gamma \langle \gamma^{-1} \rangle \to \frac{1}{2}$, $a_\gamma/a \to \infty$, because the profile $n_\gamma(r)$ sprouts a long wing at large r, which cannot be normalized. This is indicative that particles with $\gamma \overline{\gamma^{-1}} < \frac{1}{2}$ would eventually leak into the wing, and spread to $r/a \to \infty$; i.e. such particles would expand at a rate faster than the beam as a whole, making a completely self-similar solution impossible. One might expect, however, that the remaining beam would expand self-similarly, after all of the low γ particles have "evaporated" to large r.

To perform the numerical solution of Eqs. (2.35) and (2.36), we first discretize the energy distribution N_γ,

$$N_\gamma \rightarrow \sum_{i=1}^{j} N_i \, \delta(\gamma-\gamma_i). \tag{2.47}$$

We then start with an initial guess for the a_γ and solve (2.34) and (2.35), which are now reduced to a coupled set of ordinary differential equations with boundary conditions (2.32) and (2.37), by the Runge-Kutta method. We then use (2.36) to evaluate new values of the a_γ, and iterate this procedure until convergence occurs. It is convenient to choose the values of a_γ for a Bennett profile G as the initial guesses, i.e.

$$\left(\frac{a^{(0)}_\gamma}{a}\right)^2 = 2\int_0^\infty \frac{dxx}{(1+x^2)^{2\bar{\epsilon}/\epsilon_\gamma}} = \frac{1}{2\bar{\epsilon}/\epsilon_\gamma - 1} \tag{2.48}$$

This procedure usually leads to rapid convergence. In fact, the final G(x) is quite close to the Bennett shape, unless the N_γ are such as to be close to violating the requirement (2.43). This is not surprising, since G(x) is constrained to fall off as x^{-4} at $x \rightarrow \infty$.

The form of G(x) is exhibited in Fig. 1, for four different two-level (j = 2) energy distributions, summarized as cases 2-5 of Table 1. Several other features of the results are shown in Fig. 2-4. Figure 2 shows the ratio of radii, a_1/a_2, as a function of γ_1/γ_2 and N_1 (compared to the results of two approximate models discussed in Sec. III). Figure 3 shows profiles of $n_1(r)$ and $n_2(r)$, while Fig. 4 shows profiles of the total beam, $n(r) = n_1(r) + n_2(r)$.

To summarize the results of this section, we have produced an exact, completely self-similar solution to the radial beam dynamics, which holds if and only if the condition (2.43) is satisfied. We have not yet considered the time evolution that follows from an arbitrary initial specification of $n_\gamma(r)$, nor the evolution that occurs if the energy spectrum N_γ is such as to violate (2.43) for some values of γ. In Secs. III and IV, we shall use approximate models [envelope equations based on assumed forms of $n_\gamma(r)$] to attack these problems. We conclude there that the beam, with arbitrary initial conditions, does evolve toward the completely self-similar solution if (2.43) is satisfied.

C. Harmonic Magnetic Pinch and Gaussian Profiles

In this section, we consider the consequences of assuming that the magnetic pinch force $-m\gamma\omega_\beta^2(r,t)\underset{\sim}{r}$ is simple harmonic, i.e. that $\omega_\beta^2(r,t)$ is independent of r. This assumption is well satisfied near the beam axis, where the current density becomes uniform spatially. We shall find exact solutions of the Boltzmann equation, and demonstrate explicitly that the distribution $f_\gamma(r,\underset{\sim}{v},t)$ is isotropic and isothermal; these properties were only assumed in deriving the hydrodynamic equations of Sec. IIA.

For an r-independent $\omega_\beta(t)$, a function of the form

$$f_\gamma(r,\underset{\sim}{v},t) = M(t)\exp[-\tfrac{1}{2}m\gamma\omega_\beta^2 r^2\beta_r(t)-\tfrac{1}{2}m\gamma v^2\beta_v(t)-m\gamma\omega_\beta v_r r\beta_c(t)] \quad (2.49)$$

is an exact solution of the Boltzmann equation (2.1), provided that the coefficients β_r,β_v, and β_c satisfy the ordinary differential equations,

$$-\tfrac{1}{2}v^2\dot{\beta}_v-\omega_\beta\beta_c+\epsilon_\gamma\beta_r^2=0, \quad (2.50a)$$

$$-\tfrac{1}{2}m\omega_\beta^2\dot{\beta}_r - m\omega_\beta\dot{\omega}_\beta\beta_r+\epsilon_\gamma\omega_\beta^2\beta_c^2+m\omega_\beta^3\beta_c=0, \quad (2.50b)$$

$$\omega_\beta\dot{\beta}_c+\dot{\omega}_\beta\beta_c-\omega_\beta^2\beta_r+2\epsilon_\gamma\omega_\beta\beta_v\beta_c+m\omega_\beta^2\beta_v=0, \quad (2.50c)$$

and M(t) is given by the normalization,

$$N_\gamma=\int dr2\pi r\int d^2\underset{\sim}{v}\, f_\gamma(r,\underset{\sim}{v},t). \quad (2.50d)$$

Given any set of initial conditions $\beta_r(0),\beta_v(0)$, $\beta_c(0)$, the solution

is determined thereafter by Eqs. (2.50). However the initial values must satisfy the constraint

$$\beta_r(0)\beta_v(0) > \beta_c^2(0), \tag{2.51}$$

in order to permit the normalization of Eq. (2.50d). Any superposition of such solutions is also a solution, since the Boltzmann equation with a prescribed pinch force is linear in $f(r,\underset{\sim}{v},t)$.

The spatial profile determined by these solutions is Gaussian,

$$n_\gamma(r,t) \sim \exp(-r^2/a_\gamma^2(t)), \tag{2.52}$$

where

$$a_\gamma^2(t) = \left\{\tfrac{1}{2}m\omega_\beta^2[\beta_r(t)\beta_v(t) - \beta_c^2(t)]\right\}^{-1} \tag{2.53}$$

The temperature T_γ is spatially uniform,

$$T_\gamma(t) = 1/\beta_v(t), \tag{2.54}$$

and the distribution over internal velocity $\underset{\sim}{w}$ is isotropic, justifying the definition of a pressure and the neglect of heat flux. Thus these solutions satisfy all of the assumptions made in deriving the hydrodynamic equations in Sec. IIIA. Using (2.54) in the pressure balance equation (2.18), we find that T_γ is related to ω through

$$T_\gamma(t) = \tfrac{1}{2}m\gamma\omega_\beta^2 a_\gamma^2(t). \tag{2.55}$$

The assumption made in this section, that ω_β is independent of r, is only valid for the high γ beam particles, which are localized well within the characteristic beam radius a(t). It is tempting to try to develop an approximate theory by extending this assumption to all beam particles, e.g. by choosing an "average" spatially independent ω_β by requiring

$$m\gamma\omega_\beta\, a^2 = \overline{\langle m\gamma\omega_\beta^2(r) r^2\rangle} \quad . \tag{2.56}$$

With this prescription, Eq. (3.18) reduces to

$$2\,\frac{d}{dt}\,a_\gamma^{\,2} - \frac{a_\gamma^{\,2}}{a^2}\,\frac{d}{dt}\,a^2 = \frac{\epsilon_\gamma}{T_B}\,a^2. \tag{2.57}$$

Averaging (2.57) over γ yields a generalized Nordsieck equation,

$$\frac{d}{dt}\,\ell n\, a^2 = \frac{\bar{\epsilon}}{T_B}\ , \tag{2.58}$$

and using (2.58) in (2.57) gives an expression for the time dependence of $a_\gamma(t)$, given arbitrary initial values $a_\gamma(0)$,

$$a_\gamma^{\,2}(t) = \left[a_\gamma^{\,2}(0) - \frac{\epsilon_\gamma}{\bar{\epsilon}}\,a^2(0)\right]\ \exp\left(\frac{\bar{\epsilon}\,t}{2T_B}\right) + \frac{\epsilon_\gamma}{\bar{\epsilon}}\,a^2(0)\exp\left(\frac{\bar{\epsilon}t}{T_B}\right). \tag{2.59}$$

Equation (2.58) is indeed the correct generalized Nordsieck equation, derived exactly in Sec. IIB [if Eq. (2.43) is satisfied]. Equation (2.59), however, points up the deficiencies of this approximate model. The first term of (2.59) is a transient, arising out of the initial conditions. The second term, which dominates for $t \gg T_B/\bar{\epsilon}$, represents a completely self-similar beam expansion, with

all γ components expanding at the same exponential rate and such that

$$\frac{a_\gamma^2}{a_{\gamma'}^2} = \frac{\epsilon_\gamma}{\epsilon_{\gamma'}} \approx \frac{\gamma'}{\gamma} . \qquad (2.60)$$

Both Eq. (2.60) and the time scale for the decay of transients, Eq. (2.59), are essentially correct for particles with $\gamma\,\overline{\gamma^{-1}} \gg 1$. But as we have seen in Sec. IIB, such a self-similar expansion can only hold for values of γ that satisfy Eq. (2.43). The model thus fails for low γ particles; it is the very fact that the pinch force is not harmonic, but rather falls off for large r, that allows these particles to expand faster than the main beam. To calculate the time dependence of $a_\gamma(t)$ for all γ, we need a more sophisticated envelope equation (i.e. equation for a_γ) that models the pinch force more realistically. Approximate models of this type are developed in Secs. III and IV.

III. Envelope Equations

A. Derivation and General Remarks

In Sec. II, we found an exact solution of the hydrodynamic equations for the beam profiles $n_\gamma(r,t)$ and for the radial expansion rate. However the solution applied only when a restriction on the breadth of the energy distribution, Eq. (2.43), was satisfied. Furthermore, the solution applied only when the initial conditions happened to coincide with the specified form. In order to find $n_\gamma(r,t)$ with complete generality, it would be necessary to solve the general initial value problem of the hydrodynamic equations (2.18) and (2.19). We do not undertake to do that in this paper. Instead, we reduce the difficulty of the problem by going to a lower level of description. In this section, we derive envelope equations, i.e. equations determining the evolution of the characteristic radii a_γ for beam particles with a given value of γ. In order to specify the coefficients in the envelope equations, it will be necessary to assume specific functional forms for the $n_\gamma(r,t)$. Thus we obtain approximate envelope equations. However we are able to benchmark these approximate models against the exact solutions of Sec. IIB, in the regime where those solutions are valid. We are also able to solve the initial value problem for the envelope equations more generally. The results strongly indicate that the exact, completely self-similar solution of Sec. IIB is the time-asymptotic limit for any initial conditions, provided that the condition (2.43) is satisfied. Solutions are also found when (2.43) is not satisfied. In these cases, the low-γ particles expand more rapidly than the main beam.

Our starting point here is the single-particle equation of motion, and our derivation follows that of Lee and Cooper[4] for a mono-energetic beam. Under the assumptions (i-vi) of Sec. I, the equation of motion of a beam particle in the transverse plane is

$$\ddot{\underset{\sim}{r}} + \omega_\beta^2(r,t)\underset{\sim}{r} = \delta\underset{\sim}{F}/m\gamma, \tag{3.1}$$

where the betatron frequency ω_β is defined in Eq. (2.6), and $\delta\underset{\sim}{F}$ is the rapidly fluctuating stockastic force associated with Coulomb scattering off atoms in the medium. By taking the product of Eq. (3.1) with either $\underset{\sim}{r}$ or $\dot{\underset{\sim}{r}}$, and averaging <u>locally</u> over the transverse velocities $\dot{\underset{\sim}{r}}$ of beam particles with a given value of γ located in an annular volume element between and r and r + dr (denoted by $\langle\cdots\rangle_{\dot{r}}$), we arrive at the two equations

$$\frac{dV^2}{dt} + \omega_\beta^2 \left\langle \frac{dr^2}{dt} \right\rangle_{\dot{r}} = \frac{2\epsilon_\gamma}{m\gamma} , \tag{3.2}$$

$$\tfrac{1}{2} \left\langle \frac{d^2r^2}{dt^2} \right\rangle_{\dot{r}} - V^2 + \omega_\beta^2 r^2 = 0, \tag{3.3}$$

where V(r,t) is the mean or fluid velocity at r,

$$\frac{d}{dt} \equiv \frac{\partial}{\partial t} + V\frac{\partial}{\partial r} ,$$

and ϵ_γ is the rate of energy transfer to transverse motion due to scattering, given by Eq. (1.5). Eliminating V from Eqs. (3.2) and (3.3), we arrive at

$$\tfrac{1}{2} \left\langle \frac{d^3r^2}{dt^3} \right\rangle_{\dot{r}} + \left\langle \frac{d}{dt}\omega_\beta^2 r^2 \right\rangle_{\dot{r}} + \omega_\beta^2 \left\langle \frac{dr^2}{dt} \right\rangle_{\dot{r}} = \frac{2\epsilon_\gamma}{m\gamma} . \tag{3.4}$$

Next we make the assumption that the beam is in quasi-static equilibrium, i.e. that

$$\left\langle \frac{d^n r^2}{dt^n} \right\rangle_r \sim \frac{r^2}{t_{mac}^n} \ll \omega_\beta^n r^2, \tag{3.5}$$

where t_{mac} is a time characterizing macroscopic beam radial motion. This assumption means essentially that the macroscopic transverse beam dynamics is determined to lowest order by a balance between the transverse kinetic pressure and the magnetic pinch, with the scattering term on the right hand side of (3.4) leading to adiabatic beam expansion at a rate slow compared to individual particle oscillations. The first term on the left hand side of (3.4) is thus negligible*, and we complete the derivation by averaging also over position r. We obtain

$$\frac{d}{dt} \left\langle \gamma \omega_\beta^2 r^2 \right\rangle + \left\langle \gamma \omega_\beta^2 \frac{dr^2}{dt} \right\rangle = \frac{2\epsilon}{m}, \tag{3.6}$$

where $\langle \cdots \rangle$ henceforth indicates an average over (both position and

* This assumption always fails for r large enough, since the first term in (3.4) $\to r^2$, while the other terms $\to$ constant as $r \to \infty$. This is indicative that the pinch force becomes weak for beam particles that are far enough outside the main beam, and the dynamics of these particles is dominated by scattering, rather than by an equilibrium between pressure and pinch force. Thus the self-similar profiles used later are incorrect at large r -- the beam profile must approach a Gaussian shape in this region (but only at very late times). Nevertheless, the first term in (3.4) can be dropped, without significantly affecting the results in the region inside or fairly near the main beam. Once this is done, profiles such as the Bennett profile are admissable, even though they would cause the first term to diverge, because they fall off too slowly at $r \to \infty$.

velocity of) all beam particles with energy γ, i.e. for any function $g(r,t)$,

$$\langle g(r,t) \rangle \equiv N_\gamma^{-1} \int_0^\infty dr 2\pi r n_\gamma(r,t) g(r,t). \tag{3.7}$$

To proceed further, we shall assume that the functions $n_\gamma(r,t)$ are of the form

$$n_\gamma(r,t) = n_\gamma \left(\frac{r}{a_\gamma(t)} \right) , \tag{3.8}$$

i.e. that the beam particles with any single value of γ expand self-similarly. This is a much weaker assumption than the assumption made in Sec. IIB that the whole beam expands self-similarly, and we expect (3.8) to have a much broader realm of validity (e.g. when low γ particles expand faster than the main beam components). The characteristic beam radii $a_\gamma(t)$ are conveniently defined by*

$$N_\gamma \equiv \int_0^\infty dr 2\pi r n_\gamma(r,t) = \pi a_\gamma^2(t) n_\gamma(0,t), \tag{3.9}$$

and it will also be convenient later to define a characteristic radius a for the whole beam analogously,

$$1 \equiv \int_0^\infty dr 2\pi r n(r,t) = \pi a^2(t) n(0,t), \tag{3.10}$$

where $n(r,t)$ is defined in Eq. (2.5). It follows from Eq. (3.8) that

$$\langle g(r,t) \frac{1}{r^2} \frac{dr^2}{dt} \rangle = \langle g(r,t) \rangle \frac{1}{a_\gamma^2} \frac{d}{dt} a_\gamma^2 , \tag{3.11}$$

* As noted previously, it is not always possible to define a_γ as a root-mean-square radius.

for any function g(r,t). Thus Eq. (3.6) reduces to

$$\frac{d}{dt} \langle \gamma\omega_\beta^2 r^2 \rangle + \langle \gamma\omega_\beta^2 r^2 \rangle \frac{d}{dt} \ell n\, a_\gamma^2 = \frac{2\epsilon_\gamma}{m} . \tag{3.12}$$

We also note, from Eqs. (2.6) -- (2.9), and (2.20), that

$$m\gamma\omega_\beta^2 r^2 = 4T_B \int_o^r dr' 2\pi r' n(r',t), \tag{3.13}$$

and thus rewrite Eq. (3.12) in the two equivalent forms

$$\frac{d}{dt} D_\gamma(t) + D_\gamma(t) \frac{d}{dt} [\ell n\, a_\gamma^2(t)] = \frac{\epsilon_\gamma}{2T_B} , \tag{3.14a}$$

or

$$D_\gamma(t) \frac{d}{dt} \ell n\, [D_\gamma(t) a_\gamma^2(t)] = \frac{\epsilon_\gamma}{2T_B} , \tag{3.14b}$$

where

$$D_\gamma(t) \equiv N_\gamma^{-1} \int_o^\infty dr 2\pi r n_\gamma(r/a_\gamma(t)) \int_o^r dr' 2\pi r' n(r',t) \tag{3.15a}$$

$$= N_\gamma^{-1} \int_o^\infty dr 2\pi r n_\gamma(r/a_\gamma(t)) \int_o^r dr' 2\pi r' \int d\gamma' n_{\gamma'}(r'/a_{\gamma'}(t)) . \tag{3.15b}$$

Equation (3.14) is an envelope equation determining the evolution of $a_\gamma(t)$, once the coefficients $D_\gamma(t)$ are determined.

B. Small γ and Large γ Limits

Before making further assumptions to determine the coefficients $D_\gamma(t)$, we consider the limits of small γ and large γ. As in Sec. IIB, small γ will mean $2\gamma\,\overline{\gamma^{-1}} < 1$, while large γ will mean $\gamma\,\overline{\gamma^{-1}} \gg 1$. We expect, as indicated in Sec. II, that particles with large γ are confined to radii well inside a, while those with small

γ spread to well outside a (after an initial transient period). Thus, for small γ,

$$D_\gamma(t) \approx 1, \tag{3.16a}$$

and Eq. (3.14) reduces to a generalized Nordsieck equation

$$\frac{d}{dt} \ell n\, a_\gamma^2 = \frac{\epsilon_\gamma}{2T_B} \tag{3.16b}$$

for small-γ particles. We note that the expansion is exponential, at a rate inversely proportional (through T_B) to the <u>total</u> net current I_o, but inversely proportional (through ϵ_γ) to the <u>particular</u> γ of the particles. Comparing with Eq. (2.28), we expect the beam as a whole to expand roughly exponentially at a rate $\sim \bar{\epsilon}/T_B$. Thus low-γ particles, i.e. those with $\epsilon_\gamma > 2\bar{\epsilon}$ or $\gamma\,\overline{\gamma^{-1}} \leq \frac{1}{2}$, expand more rapidly, and the ratio $a_\gamma(t)/a(t)$ increases without limit.

Next we consider the limit of large γ. Since these particles are confined near the beam axis, we can take

$$n(r,t) \approx 1/\pi a^2(t), \tag{3.17}$$

i.e. the pinch force is simple harmonic in this region. As shown in Sec. IIC, this implies that

$$n_\gamma(r) = \frac{N_\gamma}{\pi a_\gamma^2(t)} \exp\left(-\frac{r^2}{a_\gamma^2(t)}\right); \tag{3.18}$$

hence

$$\langle r^2 \rangle = a_\gamma^2. \tag{3.19}$$

We do not need to use Eq. (3.18) here, but we do use the fact that $\langle r^2 \rangle$ is finite, Eq. (3.19). Using (3.17) in (3.15a), we then find

$$D_\gamma(t) \approx a_\gamma^2(t)/a^2(t). \tag{3.20}$$

Equation (3.14) then has a solution with

$$\frac{a_\gamma^2(t)}{a^2(t)} = \frac{\epsilon_\gamma}{2T_B \frac{d}{dt} \ell n\, a^2}\ , \tag{3.21}$$

i.e. the large-γ beam components expand at essentially the same rate as the main beam, but their characteristic radii scale as $\epsilon_\gamma^{1/2}$, i.e. as $\gamma^{-1/2}$.

C. Approximate Envelope Equation Model

In order to evaluate the coefficients $D_\gamma(t)$ in the envelope equation (3.14), without knowing the general form of the profiles $n_\gamma(r)$, we shall consider some ad hoc assumed forms for $n_\gamma(r)$. The validity of these assumptions can be tested, to some extent, by comparison with the exact, completely self-similar solution of Sec. IIB, which hold when condition (2.43) is satisfied.

We consider three very different self-similar forms $n_\gamma(r/a_\gamma(t))$:

$$\text{(Case i)}\quad n_\gamma(r,t) = \frac{N_\gamma}{\pi a_\gamma^2(t)} \exp\left(-\frac{r^2}{a_\gamma^2(t)}\right), \tag{3.22a}$$

$$\text{Case ii)}\quad n_\gamma(r,t) = \frac{N_\gamma}{\pi a_\gamma^2(t)} \left(1 + \frac{r^2}{a_\gamma^2(t)}\right)^{-2}, \tag{3.22b}$$

$$\text{(Case iii)}\quad n_\gamma(r,t) = \frac{N_\gamma}{\pi a_\gamma^{\,2}(t)}\left(1+\frac{r^2}{r_o^{\,2}(t)}\right)^{-1-r_o^{\,2}(t)/a_\gamma^{\,2}(t)}. \tag{3.22c}$$

Case (i) is the Gaussian profile, correct for large γ. Case (ii) is the Bennett profile, correct for a mono-energetic beam[3]. Case (iii) was chosen by analogy with the exact self-similar solution (2.33) with the approximation $G(x) = (1 + r^2/r_o^{\,2})^{-2}$, the Bennett form. The exponent used in Eq. (3.22c) is required to satisfy the normalization (2.3). The parameter $r_o(t)$ is a γ-independent radius, which is left arbitrary; the resulting envelope equations turn out to be independent of the choice of $r_o(t)$.

Most remarkably, all three cases share the property that

$$D_\gamma(t) = \int d\gamma'\, N_{\gamma'}\, \frac{a_\gamma^{\,2}}{a_\gamma^{\,2} + a_{\gamma'}^{\,2}}. \tag{3.23}$$

The generality of this results tempts one to speculate that it is a general consequence of all profiles of the form $n_\gamma(r/a_\gamma(t))$. The reader is warned that this is not so.

Using (3.23) is (3.14), we obtain an integral-differential equation for a_γ:

$$\frac{d}{dt}\int d\gamma'\, N_{\gamma'}\, \frac{a_\gamma^{\,2}}{a_\gamma^{\,2} + a_{\gamma'}^{\,2}} + \frac{da_\gamma^{\,2}}{dt}\int d\gamma'\, N_{\gamma'}\, \frac{1}{a_\gamma^{\,2} + a_{\gamma'}^{\,2}}\frac{\epsilon_\gamma}{2T_B}, \tag{3.24a}$$

or

$$\int d\gamma'\, N_{\gamma'}\, \frac{a_\gamma^{\,2}}{a_\gamma^{\,2} + a_{\gamma'}^{\,2}}\,\frac{d}{dt}\ln\int d\gamma' N_{\gamma'}\, \frac{a_\gamma^{\,4}}{a_\gamma^{\,2} + a_{\gamma'}^{\,2}} = \frac{\epsilon_\gamma}{2T_B} \tag{3.24b}$$

We look first for solutions of (3.24) that are completely self-similar, i.e. such that the ratio $a_\gamma/a_{\gamma'}$ is constant in time, or

equivalently

$$\frac{d}{dt} \ell n\, a_\gamma^2 = \frac{d}{dt} \ell n\, a^2, \text{ for all } \gamma. \tag{3.25}$$

Equation (3.24) then reduces to

$$\int d\gamma' N_{\gamma'} \frac{a_\gamma^2}{a_\gamma^2 + a_{\gamma'}^2} \frac{d}{dt} \ell n\, a^2 = \frac{\epsilon_\gamma}{2T_B} . \tag{3.26}$$

Multiplying by N_γ and integrating, we find

$$\frac{d\, \ell n\, a^2}{dt} \int d\gamma N_\gamma \int d\gamma' N_{\gamma'} \frac{a_\gamma^2}{a_\gamma^2 + a_{\gamma'}^2} = \frac{d\, \ell n\, a^2}{dt} \int d\gamma\, N_\gamma \int d\gamma'\, N_{\gamma'} \frac{\frac{1}{2}(a_\gamma^2 + a_{\gamma'}^2)}{a_\gamma^2 + a_{\gamma'}^2}$$

$$= \tfrac{1}{2} \frac{d}{dt} \ell n\, a^2 = \frac{\bar{\epsilon}}{2T_B} .$$

Thus we arrive at the same generalized Nordsieck equation derived exactly in Sec. IIB,

$$\frac{d}{dt} \ell n\, a^2 = \frac{d}{dt} \ell n\, a_\gamma^2 = \frac{\bar{\epsilon}}{T_B} , \tag{3.27}$$

which helps to establish our confidence in the assumptions (3.22) that led to Eq. (3.23). Using (3.27) in (3.26), we find

$$\int d\gamma' N_{\gamma'} \frac{a_\gamma^2}{a_\gamma^2 + a_{\gamma'}^2} = \frac{\epsilon_\gamma}{2\bar{\epsilon}} \approx \frac{1}{2\gamma\sqrt{\gamma^2 - 1}} . \tag{3.28}$$

The integral equation (3.28) determines the relative magnitude of the various a_γ. For example, if the energy distribution N_γ is discretized,

$$N_\gamma = \sum_{i=1}^{j} N_i \delta(\gamma - \gamma_i), \tag{3.29}$$

then Eq. (3.28) becomes a set of j algebraic equations (one of which is redundant),

$$\sum_{k=1}^{j} N_k \frac{a_i^2}{a_i^2 + a_k^2} = \frac{\epsilon_i}{2\bar{\epsilon}} \approx \frac{1}{2\gamma_i \overline{\gamma^{-1}}} , \tag{3.30}$$

that determine the j-1 unknowns a_2/a_1, a_3/a_1,...,a_j/a_1. Also, a_1 is determined by its initial value and Eq. (3.27).

Since the left hand side of Eq. (3.28) or (3.30) is less than unity, a necessary condition for the existence of a completely self-similar solution of Eq. (3.24) is

$$\frac{\bar{\epsilon}}{\epsilon_\nu} \approx \nu\,\overline{\nu^{-1}} > \tfrac{1}{2}, \text{ for all } \nu. \tag{3.31}$$

We proved in Sec. IIB that condition (3.31) is both necessary and sufficient for a completely self-similar exact solution of the hydrodynamic equations. However, Eq. (3.31) is not sufficient within the framework of the approximate model, Eq. (3.24). This indicates a defect in the approximate model, which, we find, agrees well with the exact solution if (3.31) is well satisfied.

To illustrate this, we consider a two level discrete energy distribution, j = 2 in Eq. (3.29), as we did in Sec. IIB. Equations (3.30) can then be solved for a_2/a_1, with the result

$$\frac{a_1^2}{a_2^2} = \frac{\bar{\epsilon} + \epsilon_1 - \epsilon_2}{\bar{\epsilon} - \epsilon_1 + \epsilon_2} = \frac{(2-N_2) - \epsilon_2/\bar{\epsilon}}{(2-N_1) - \epsilon_1\bar{\epsilon}} \quad . \tag{3.32}$$

The condition for the solution to be physical is that a_1^2/a_2^2 be positive and finite, which requires that

$$\frac{\bar{\epsilon}}{\epsilon_1} \approx \overline{\nu^{-1}}\,\nu_1 > \frac{1}{2-N_1}\,, \tag{3.33}$$

if $\nu_1 < \nu_2$. Comparing with Eq. (3.31), we see that (3.33) is a stronger requirement. Solutions of Eq. (3.32) have been plotted in Fig. 2, as well as plots of a_1/a_2 from the exact theory of Sec. IIB. We see that agreement between the two is good where (3.33) is well satisfied. This is to be expected, since we showed in Sec. IIB that the exact form of $n_\nu(r,t) = \frac{N_\nu}{\pi a_\nu^2}\,[G(r/a)]^{\bar{\epsilon}/\epsilon_\nu}$ is close to one of the approximate

forms, Eq. (3.22c), that leads to the present model. However, near the region of breakdown of the completely self-similar solution, the value of a_1/a_2 is evidently sensitive to features of the profile $n_\gamma(r,t)$ that cannot be modeled as in Eq. (3.22c).

We turn next to the general initial value problem for Eqs. (3.24), given arbitrary initial values for a_γ. When N_γ is discretized, as in Eq. (3.29), Eq. (3.24) becomes a set of j coupled ordinary differential equations in the variables $a_i(t)$, $1 \le i \le j$, which can be solved numerically in straightforward ways. We consider again the two-level discrete distribution in γ, for which the following analytic solution can be found, after much tedious algebra:

$$\left[\frac{a_1^2(t)}{a_1^2(0)}\right]^{N_1^2}\left[\frac{a_2^2(t)}{a_2^2(0)}\right]^{N_2^2}\left[\frac{a_1^2(t)+a_2^2(t)}{a_1^2(0)+a_2^2(0)}\right]^{2N_1N_2} = \exp\left(\frac{\bar{\epsilon}t}{T_B}\right), \tag{3.34}$$

$$\left[\frac{a_1^2(t)/a_2^2(t)}{a_1^2(0)/a_2^2(0)}\right]^{P}\left[\frac{a_1^2(t)/a_2^2(t)+1}{a_1^2(0)/a_2^2(0)+1}\right]^{Q}\left[\frac{a_1^2(t)/a_2^2(t)-S}{a_1^2(0)/a_2^2(0)-S}\right]^{R} = \exp\left(\frac{\bar{\epsilon}t}{T_B}\right) \tag{3.35}$$

where

$$P \equiv \frac{N_1(1+N_1)\bar{\epsilon}}{\bar{\epsilon}+\epsilon_1-\epsilon_2}, \tag{3.36}$$

$$Q \equiv 1 + 2N_1N_2, \tag{3.37}$$

$$R \equiv \frac{(\epsilon_1-\epsilon_2)^2(2N_1N_2+1)+2(\epsilon_1-\epsilon_2)\bar{\epsilon}(N_1-N_2)-3\bar{\epsilon}^2}{\bar{\epsilon}^2-(\epsilon_1-\epsilon_2)^2}, \tag{3.38}$$

$$S \equiv \frac{\bar{\epsilon} + \epsilon_1 - \epsilon_2}{\bar{\epsilon} - \epsilon_1 + \epsilon_2} . \tag{3.39}$$

This complicated solution can be shown to have the following properties: (i) If condition (3.33) is satisfied, it tends asymptotically to the completely self-similar solution of Eqs. (3.27) and (3.32). (ii) If condition (3.33) is not satisfied, then $a_1(t)$ and and $a_2(t)$ tend asymptotically toward exponential expansion, but at different rates, with $a_1(t)$ expanding faster:

$$\frac{d}{dt} \ell n\, a_1^2 = \frac{\epsilon_1}{(1 + N_2)T_B} , \tag{3.40a}$$

$$\frac{d}{dt} \ell n\, a_2^2 = \frac{(N_2 - N_1)\epsilon_2}{N_2\, T_B} . \tag{3.40b}$$

(iii) If condition (3.33) is not satisfied, and $N_1 \ll 1$ (so that the beam component with $\gamma = \gamma_2$ represents the "main beam"), then asymptotically in time a_2 expands as if only the $\gamma = \gamma_2$ part of the beam were there,

$$a_2^2(t) \xrightarrow[t \to \infty]{} \exp\left(\frac{\epsilon_2 t}{T_B}\right), \tag{3.41}$$

while a_1 expands as discussed in Sec. IIIB,

$$a_1^2(t) \xrightarrow[t \to \infty]{} \exp\left(\frac{\epsilon_1 t}{2T_B}\right). \tag{3.42}$$

(iv) The time scale for the approach to these asymptotic limits is typically several times the time scale for beam expansion, $T_B/\bar{\epsilon}$. Thus transient effects remain important until the beam has

expanded considerably from its initial radius.

All of these features are illustrated in Fig. 5, where the time evolution of various quantities is shown, for Cases 1, 3, 4, and 5 of Table 1. The initial condition $a_1(0) = a_2(0)$ is used for all cases. Plotted are the characteristic beam radius a(t), in the form of the ratio of $a^2(t)$ to the value

$$a_o^2(t) \equiv a^2(0) \exp(\bar{\epsilon}t/T_B) \tag{3.43}$$

predicted by the Nordsieck equation (2.28) for the completely self-similar case, and the ratio $a_1(t)/a_2(t)$. (Also shown are several results of the model discussed in Sec. D.) It is seen that $a^2(t)/a_o^2(t)$ is less than unity by a value that ranges from a few percent to ~ 30%, during a period when $a^2(t)$ e-folds many times. Thus we conclude that Eq. (2.28) is quite an accurate representation of overall beam expansion, even during the transient stage, and even for distributions N_γ that violate the requirement (2.43) for the existence of a completely self-similar solution.

We note that the definition of a "characteristic beam radius" is to some extent arbitrary for a multi-level distribution N_γ, since the radial beam profile n(r,t) will have plateaus and wings, and in general differ from a typical bell-shaped curve. This effect is most pronounced for the two level distributions discussed here. The definition of a in Eq. (3.10) essentially reflects the evolution of the on-axis density Nn(r = 0, t), a quantity of particular interest. Other definitions of a "characteristic" beam radius would exhibit somewhat

different behavior, e.g. a mean-square radius, defined by

$$a_{MS}^2(t) = \Sigma N_i a_i^2(t),$$

would be larger than $a_o^2(t)$, by a few percent to a few tens of percent, over the same time scale shown in Fig. 5.

In general, the model discussed in this section appears to give reasonable results, except for the time-asymptotic results in the sensitive regime near the limits of applicability of the completely self-similar solution. Thus we regard it as a useful model for approximate calculations. In the next section, however, we develop a model that is further simplified and easily solved, which retains many of the desirable features.

D. Simpler Envelope Model

In this section, we consider a simpler and more approximate model, within which it is possible to solve the general initial value problem for $a_\gamma(t)$ in closed form for any distribution N_γ (discrete or continuous). The model gives the exact condition (2.43) for the existence of a completely self-similar solution, and in many cases agrees well with the ratios a_γ/a_γ' for the exact, completely self-similar solution, and with the time evolution found in the last section. We start by continuing to assume that $n_\gamma(r/a_\gamma)$ takes one of the forms of Eqs. (3.22a, b, or c), but we adopt the simpler assumed form for the total beam density profile,

$$\text{(Case i)} \qquad n(r,t) = \frac{1}{\pi a^2(t)} \exp\left(-\frac{r^2}{a^2(t)}\right), \qquad (3.44a)$$

(Case ii) $$n(r,t) = \frac{1}{\pi a^2(t)} \frac{1}{[1 + r^2/a^2(t)]^2} , \tag{3.44b}$$

(Case III) $$n(r,t) = \frac{1}{\pi a^2(t)} \left(1 + \frac{r^2}{r_o^2(t)}\right)^{-1-r_o^2(t)/a^2(t)} , \tag{3.44c}$$

rather than by using the self-consistent prescription,

$$n(r,t) = \int d\gamma\, n_\gamma(r,t). \tag{3.45}$$

The choices (3.44), particularly (3.44a) and (3.44b) are obviously suggested approximate forms. In all three cases, we have then from Eq. (3.15a),

$$D_\gamma(t) = \frac{a_\gamma^2}{a_\gamma^2 + a^2} , \tag{3.47}$$

instead of Eq. (3.23). Substituting in Eq. (3.14), $a_\gamma(t)$ is determined, in terms of $a(t)$, by the ordinary differential equation,

$$\frac{a_\gamma^2}{a_\gamma^2 + a^2} \frac{d}{dt} \ell n \frac{a_\gamma^4}{a_\gamma^2 + a^2} = \frac{\epsilon_\gamma}{2T_B} , \tag{3.48}$$

instead of the integral-differential equation (3.24). Letting

$$y_\gamma(t) \equiv a_\gamma^2(t)/a^2(t), \tag{3.49}$$

Eq. (3.48) can be put in the form

$$\frac{dy_\gamma}{dt} = \left(\frac{\epsilon_\gamma}{2T_B} - \frac{y_\gamma}{1 + y_\gamma} \frac{d}{dt} \ell n\, a^2 \right) \frac{(1 + y_\gamma)^2}{2 + y_\gamma} . \tag{3.50}$$

Clearly, a completely self-similar solution, i.e. one with

$$\dot{y}_\gamma = 0, \quad \text{all } \gamma, \tag{3.51}$$

can occur if and only if

$$\frac{d}{dt} \ell n\, a^2 = \text{constant}, \tag{3.52}$$

and

$$y_\gamma = \left(\frac{2T_B}{\bar{\epsilon}_\gamma} \frac{d}{dt} \ell n\, a^2 - 1 \right)^{-1} . \tag{3.53}$$

Since there does not appear to be any obvious way to calculate $\dot{a}$ within this simple model (e.g. by setting a equal to some obviously appropriate average of a_γ), we appeal to the exact self-similar solution of Sec. IIB, which gave

$$\frac{d}{dt} \ell n\, a^2 = \frac{\bar{\epsilon}}{T_B} . \tag{3.54}$$

Using Eq. (3.54) in Eq. (3.53) gives

$$y_\gamma \equiv \frac{a_\gamma^2}{a^2} = \frac{1}{2\bar{\epsilon}/\epsilon_\gamma - 1} \approx \frac{1}{2\gamma\,\overline{\gamma^{-1}} - 1} . \tag{3.55}$$

Equation (3.55) has the correct qualitative properties of the exact completely self-similar solution derived in Sec. IIB, i.e.: First, the solution exists if and only if

$$\bar{\epsilon}/\epsilon_\gamma \approx \gamma\,\overline{\gamma^{-1}} > \tfrac{1}{2}, \text{ for all } \gamma. \tag{3.56}$$

Second,

$$a_\gamma \to \infty, \text{ for } \bar{\epsilon}/\epsilon_\gamma \to \tfrac{1}{2} . \tag{3.57}$$

Third,

$$a_\gamma \propto \epsilon_\gamma^{\frac{1}{2}} \sim \gamma^{-\frac{1}{2}}, \text{ for } \gamma\sqrt{\gamma^{-1}} \gg 1 \quad , \tag{3.58}$$

as shown in Secs. IIC and IIIB. Fourth a_γ is a monotonically decreasing function of γ, in the range of applicability, $\gamma\sqrt{\gamma^{-1}} > \frac{1}{2}$. Plots of Eq. (3.55) for two-level distributions N_γ, shown in Fig. 2, agree well with the exact solutions when $\gamma_1/\gamma_2 \geq 0.5$, but not for $\gamma_1/\gamma_2 = 0.25$. The latter is a very severe test. For actual continuous distributions N_γ, the beam profile n(r) will have a smoother shape, as assumed in Eqs. (3.44), and we would expect the model to give accurate results for y_γ. Equation (3.55) can, of course, also be applied with ease to continuous or multi-level discrete distributions N_γ, for which the exact solutions become time-consuming and rather unilluminating.

We consider next the solution of Eq. (3.50), with general initial conditions, in several limits. We note first that, if and only if Eq. (3.56) holds, the solution to Eq. (3.50), with any initial conditions, asymptotically approaches the completely self-similar solution, Eq. (3.55). This assures us once again that the latter is the physically significant solution. If inequality (3.56) is strongly satisfied and $y \ll 1$, Eq. (3.50) reduces to the linear equation

$$\frac{dy_\gamma}{dt} = \frac{\epsilon_\gamma}{4T_B} - \tfrac{1}{2}\, y_\gamma \frac{d}{dt} \ell n\, a^2, \tag{3.59}$$

whose general solution is

$$y_\gamma = \frac{\epsilon_\gamma}{2T_B}\left(\frac{d}{dt}\ell n\, a^2\right)^{-1} + \left[y_\gamma(0) - \frac{\epsilon_\gamma}{2T_B}\left(\frac{d}{dt}\ell n\, a^2\right)^{-1}\right]\exp\left(-\tfrac{1}{2}t\frac{d}{dt}\ell n\, a^2\right). \tag{3.60}$$

Equation (3.60) reproduces the solution (2.59) found in Sec. IIC. As a final limiting case, if Eq. (3.56) fails for a particular value of γ, then Eq. (3.50) shows that $y_\gamma \to \infty$, and moreover that for $y_\gamma \gg 1$,

$$\frac{d}{dt}\ell n\, y_\gamma \approx \frac{\epsilon_\gamma}{2T_B} - \frac{d}{dt}\ell n\, a^2, \tag{3.61}$$

so that, from definition (3.49),

$$\frac{d}{dt}\ell n\, a_\gamma^{\,2} \approx \frac{\epsilon_\gamma}{2T_B}, \tag{3.62}$$

in agreement with the generalized Nordsieck equation (3.16) derived in Sec. IIIB for large γ.

If (in the spirit of a first iteration), we use Eq. (3.54) in (3.50), even when the solution is not completely self-similar, then the <u>general</u> initial value problem (3.50) for $y_\gamma(t)$ can be solved in the closed form,

$$\frac{\bar{\epsilon}}{T_B}\, t = \ell n\left(\frac{y_\gamma(t)+1}{y_\gamma(0)+1}\right) - \frac{A-1}{A}\ell n\,\frac{A[y_\gamma(t)+1]+1}{A[y_\gamma(0)+1]+1}, \tag{3.63}$$

where

$$A \equiv -1 + (2\gamma\sqrt{\gamma-1})^{-1}. \tag{3.64}$$

The solution (3.63) involves the distribution N_γ only through $\bar{\epsilon}$, and

thus can be applied to any form of N_γ. Plots of $y_\gamma(t)$, $a_1^2(t)/a_2^2(t)$, and $a^2(t)/a_0^2(t)$ are shown in Fig. 5, for the two-level discrete distributions of Table 1, Cases 1, 3, 4, 5. We recall that $a^2(t)$ and $a_0^2(t)$ are as defined in Eqs. (3.10) and (3.43), i.e.

$$\frac{a^2(t)}{a_0^2(t)} \equiv \left(\frac{N_1}{y_1} + \frac{N_2}{y_2} \right)^{-1} , \tag{3.65}$$

$$\frac{a_1^2(t)}{a_2^2(t)} \equiv \frac{y_1(t)}{y_2(t)} . \tag{3.66}$$

We note the excellent quantitative agreement between the results of the present model and that of Sec. IIIC. It is particularly striking that even in Case C, Fig. 5b, the asymptotic values of a_1^2/a_2^2 for the two models differ, but the time evolution is nonetheless almost identical for a very long time.

IV. Conclusions

We have shown that if the energy distribution of a self-pinched, relativistic beam is such that

$$\bar{\epsilon}/\epsilon_\gamma \approx \gamma\,\overline{\gamma^{-1}} > \tfrac{1}{2} \tag{4.1}$$

for all beam particles, then the beam expands, under the influence of scattering by the medium, in a completely self-similar manner after an initial transient stage. In this case, the expansion was shown to be at the rate

$$\frac{d}{dt}\ell n\, a^2 = \frac{\bar{\epsilon}}{T_B}\,, \tag{4.2}$$

and exact solutions were found for the radial profiles $n_\gamma(r/a(t))$, such that higher-energy particles are more localized near the beam axis. Typically Eq. (4.1) is violated if the energy distribution N_γ has a low-amplitude tail at small γ. Particles which strongly violate the inequality (4.1) were shown to expand more rapidly than the main beam, at a rate that tends asymptotically to

$$\frac{d}{dt}\ell n\, a_\gamma^{\,2} = \frac{\epsilon_\gamma}{2T_B}\,. \tag{4.3}$$

Two different approximate envelope equation models, of distinct levels of sophistication and mathematical complexity, were developed to determine the evolution of $a_\gamma(t)$, the characteristic radius for particles with energy $mc^2\gamma$. The models were benchmarked against the exact results, where applicable. The general initial value problem was studied for each of the envelope models. The most important

conclusions were that a significant time, typically a few times $\bar{\epsilon}/T_B$, is necessary to approach the asymptotic limits discussed above; that the generalized Nordsieck equation (4.2) is quite accurate even during this period, if (4.1) holds; that the expansion rate of a [defined by Eq. (3.10) as a radius that characterizes the beam in the sense that a^2 is inversely proportional to the on-axis density] is less than or equal to Eq. (4.2), but the disparity becomes large only if (4.1) is violated and $\bar{\epsilon}t/T_B \geq 2$. In general, the nature of the evolution is that very low energy particles "evaporate" by rapid radial expansion, while the main beam expands more or less according to Eq. (4.2).

The principal assumption made was that the energy of any given beam particle is constant (although an initial energy spread among different particles was assumed). It would be straightforward to include deterministic energy losses in these calculations, but difficult to include, self-consistently, statistical energy loss mechanisms such as bremsstrahlung emission, which continuously increase the energy spread. In general, we expect that the effect of such mechanisms would be to continuously generate low-energy particles, which evaporate, thus slowly reducing the effective net current. In addition, the left hand side of the generalized Nordsieck equations would be modified in a way discussed by Lee and Cooper[4], i.e. $(d/dt)\, \ell n\, a_\gamma^2$ would be replaced by $(d/dt)\, \ell n\, (\gamma a_\gamma^2)$. Otherwise we do not expect that the main conclusions of this paper would be changed markedly, although a quantitative study of the effects would be quite interesting.

ACKNOWLEDGMENTS

We are pleased to acknowledge that discussions with Robert Biegalski contributed to the evolution of these ideas. This work was supported in part by Naval Surface Weapons Center.

REFERENCES

1. W. H. Bennett, Phys. Rev. 45, 890 (1934).
2. L. Spitzer, "Physics of Fully Ionized Gases", Second Edition, Interscience, New York, 1962, p. 109.
3. E. P. Lee, Phys. Fluids 19, 160 (1976).
4. E. P. Lee and R. K. Cooper, Particle Accel. 7, 83 (1975).
5. A. Nordsieck (deceased), unpublished.
6. J. D. Jackson, "Classical Electrodynamics", Wiley, New York, 1962, Chap. 13.

Table 1

Case	N_1	N_2	γ_1/γ_2	$\gamma_1\overline{\gamma^{-1}}$	$\gamma_2\overline{\gamma^{-1}}$
1	0.2	0.8	0.25	0.4	1.6
2	0.2	0.8	0.5	0.6	1.2
3	0.8	0.2	0.25	0.85	3.4
4	0.5	0.5	0.5	0.75	1.5
5	0.5	0.5	0.75	0.875	1.167

Some two level distributions that are used as examples in our numerical calculations.

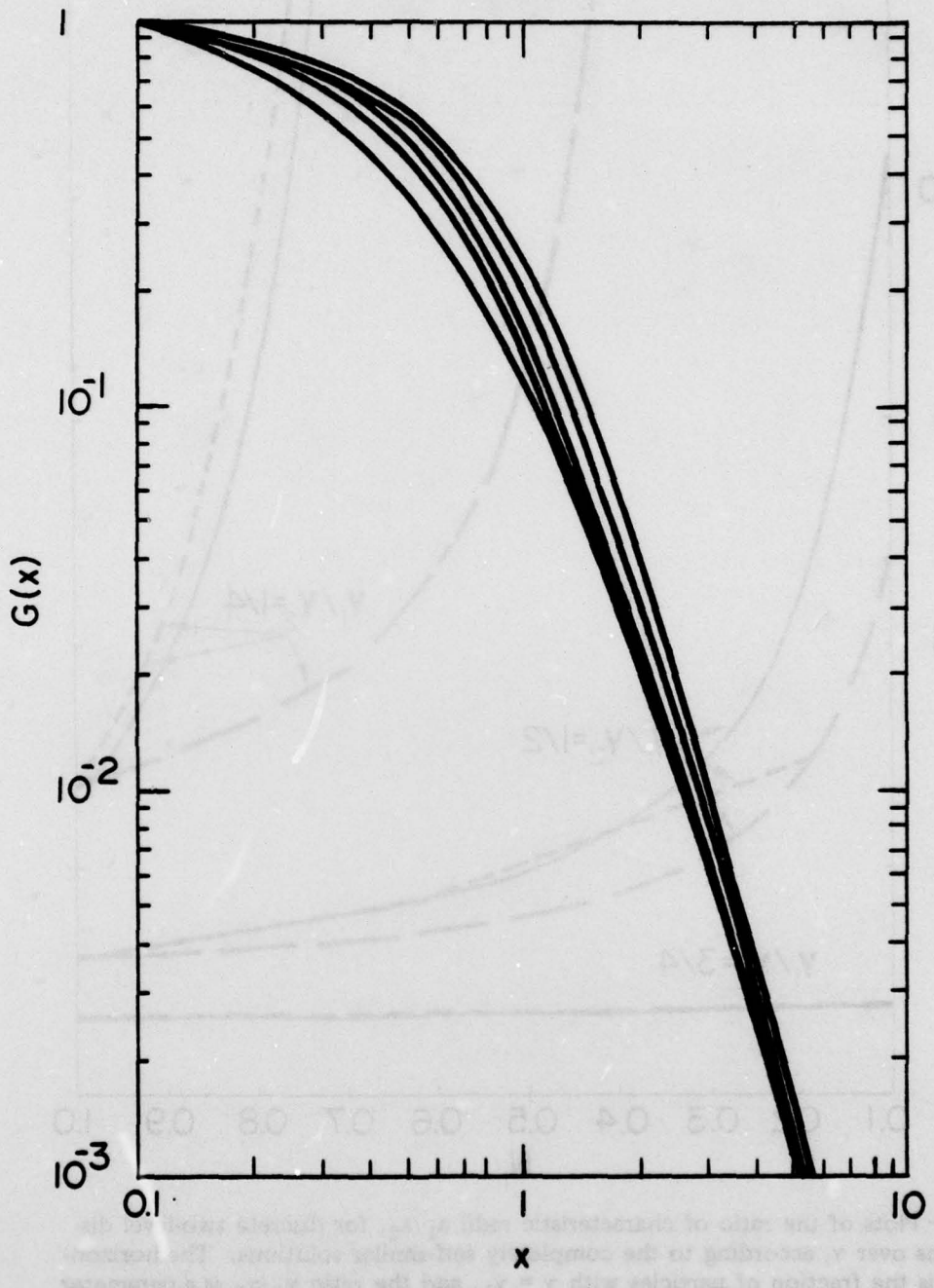

Fig. 1 — Plots of the function G(x) for several cases. The uppermost curve is a Bennett profile, included for comparison. The other curves, reading down from the top, are G(x) for Cases 5, 2, 4, and 3 of Table 1.

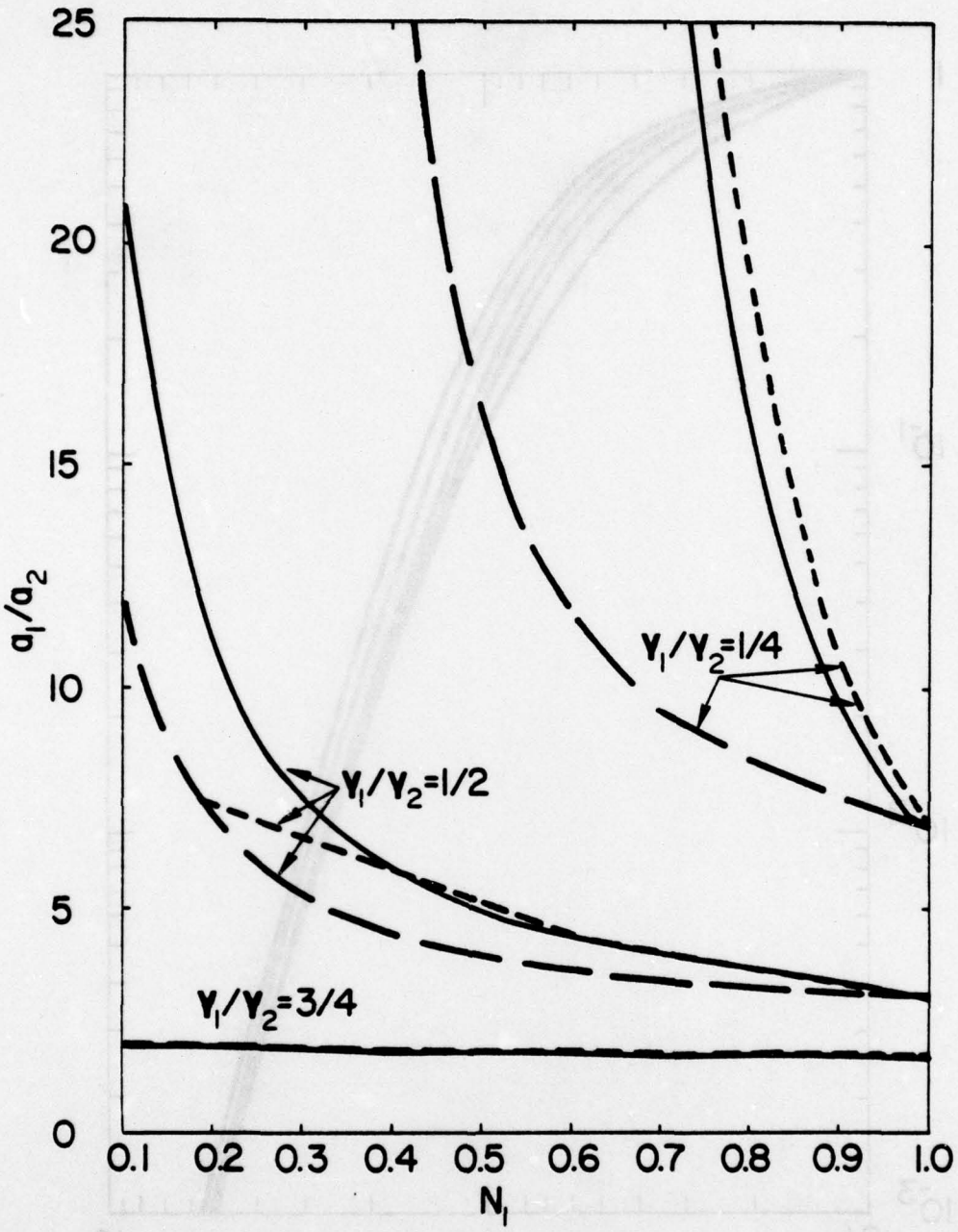

Fig. 2 — Plots of the ratio of characteristic radii a_1/a_2, for discrete two-level distributions over γ, according to the completely self-similar solutions. The horizontal axis is the fraction of particles with $\gamma = \gamma_1$, and the ratio γ_1/γ_2 is a parameter with the values 0.75, 0.5, and 0.25. The short-dashed curves are the exact solutions of Sec. IIB, the solid curves are the approximate results of Eq. (3.32), and the long-dashed curves are the approximate results of Eq. (3.55). For γ_1/γ_2 = 0.75, the three curves are virtually indistinguishable.

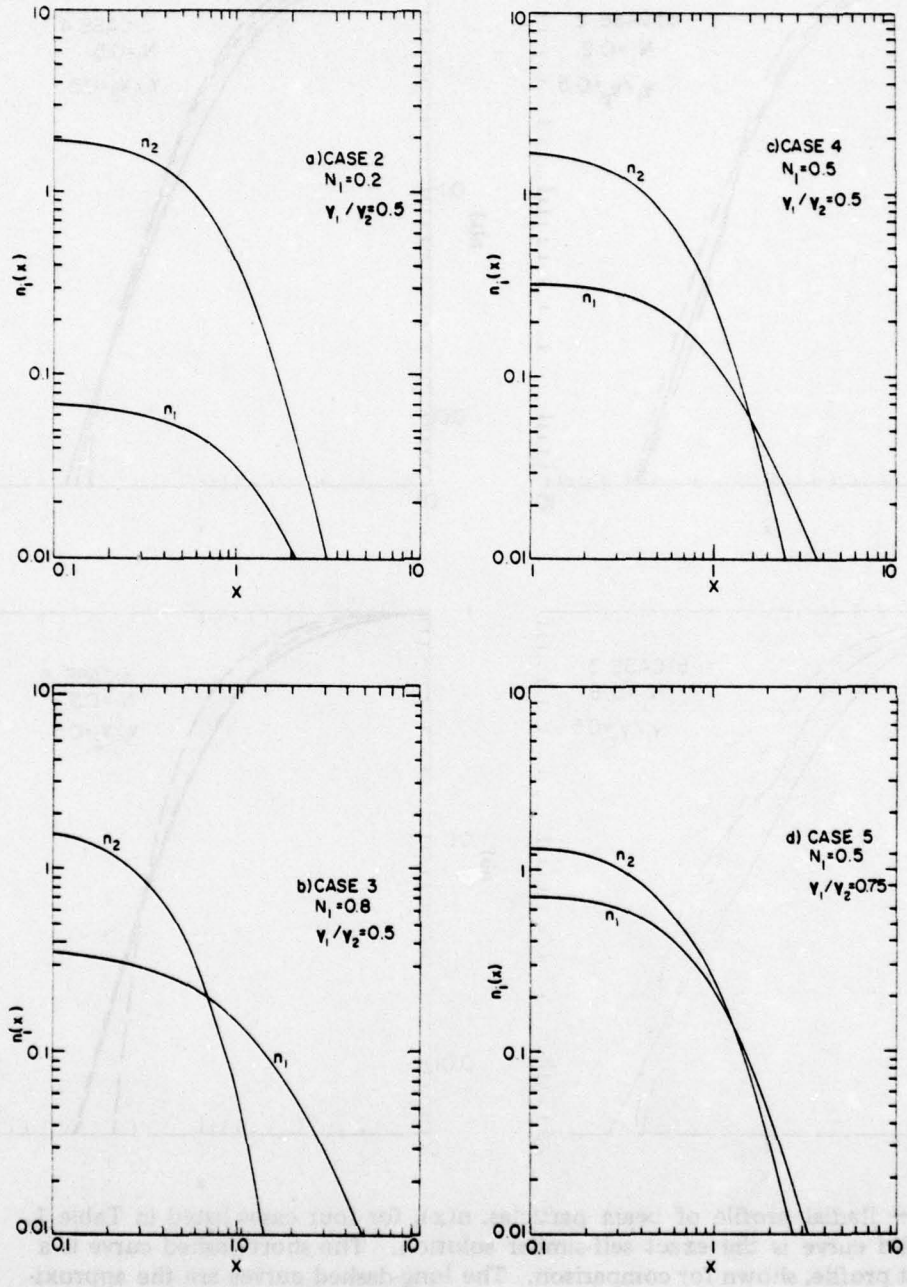

Fig. 3 — Radial profile of each of the two energy components, $n_1(x)$ and $n_2(x)$, according to the exact self-similar solution, for four cases listed in Table 1.

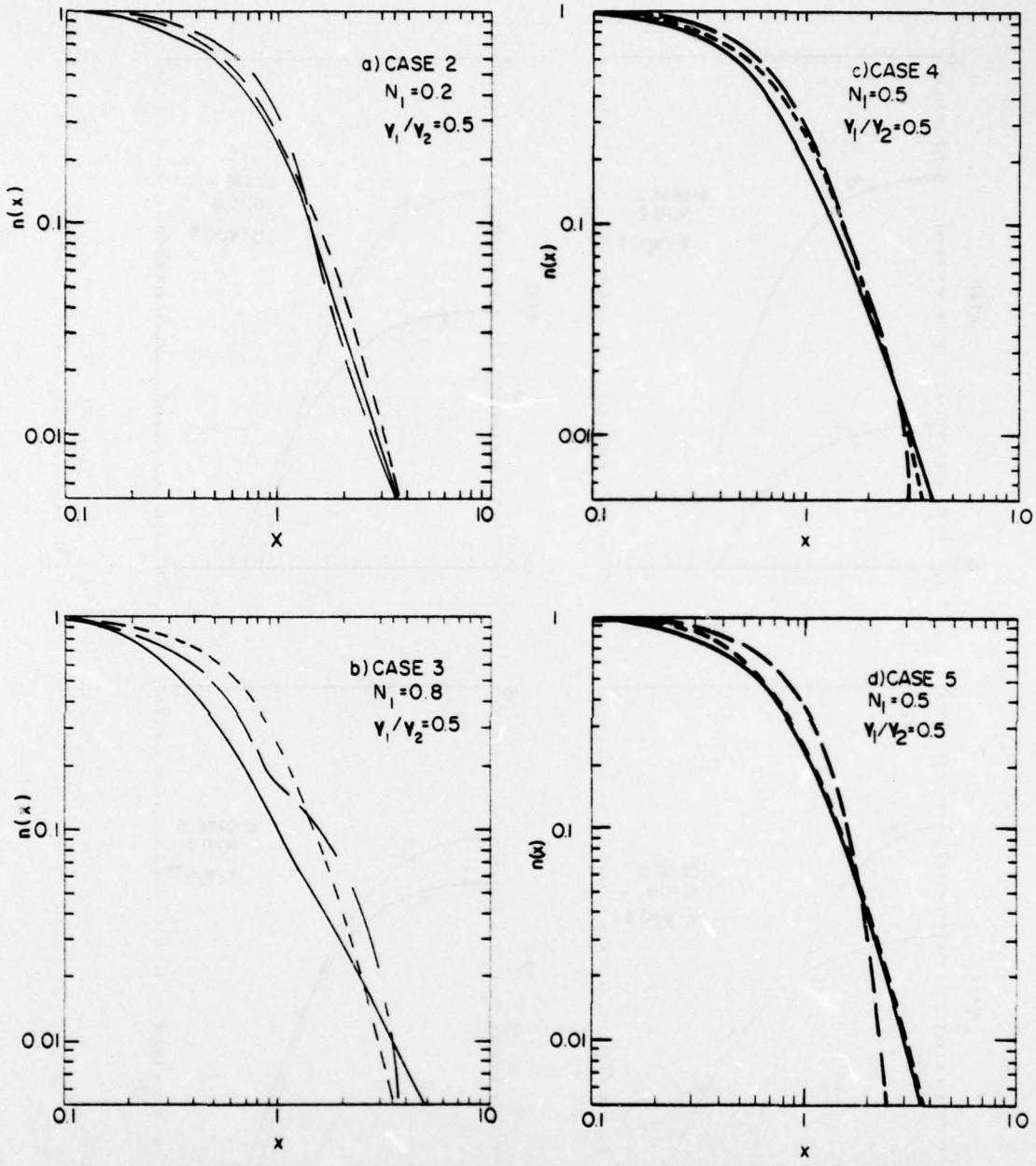

Fig. 4 — Radial profile of beam particles, n(x), for four cases listed in Table 1. The solid curve is the exact self-similar solution. The short-dashed curve is a Bennett profile, shown for comparison. The long-dashed curves are the approximate results of Eq. (3.32), with the additional assumption that the profiles of each of the two energy components, $n_1(x)$ and $n_2(x)$, are Gaussian.

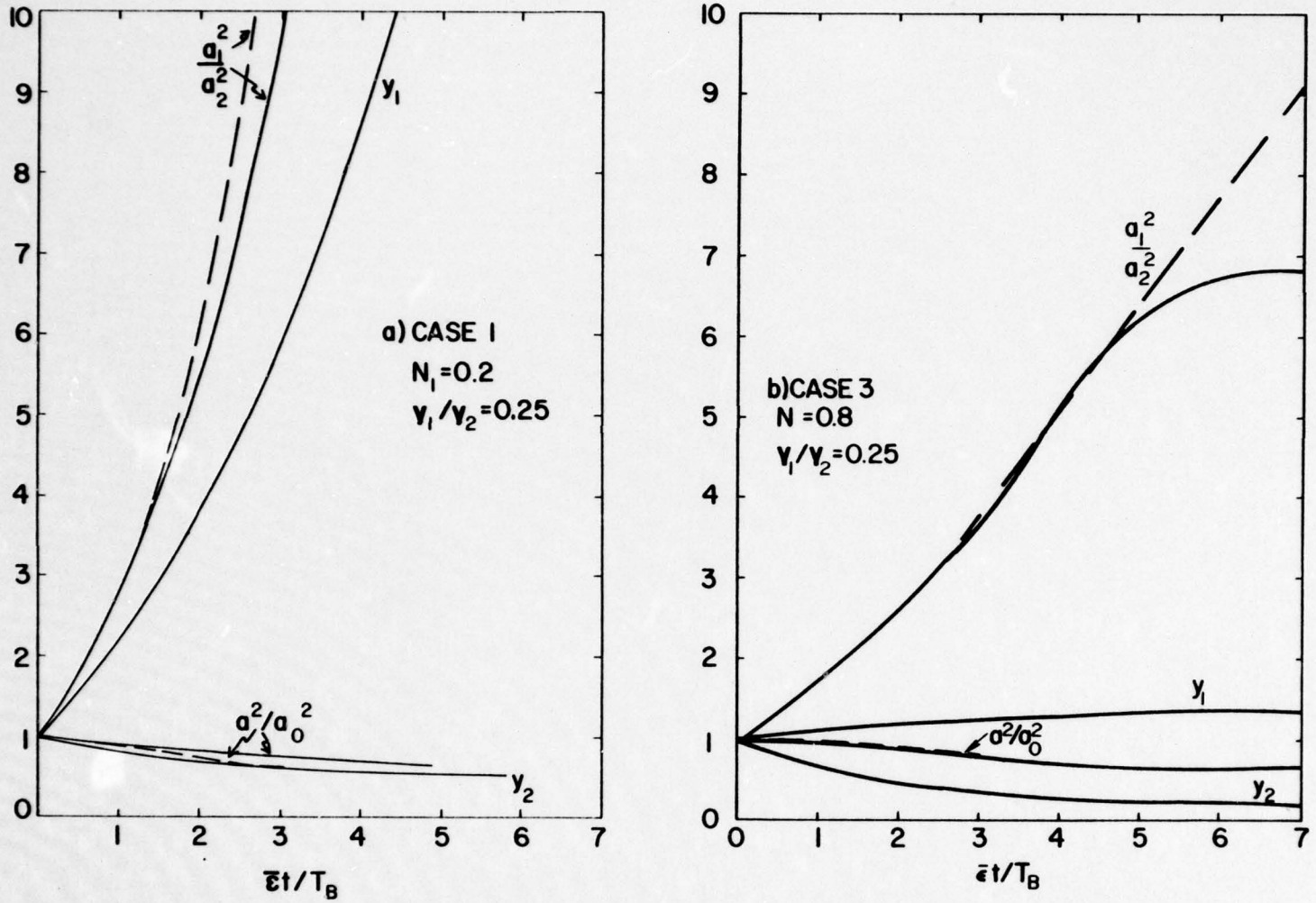

Fig. 5 — Time dependence of the quantities a_1^2/a_2^2, a^2/a_0^2, y_1, and y_2, for four different cases listed in Table 1. Dashed curves are results from the model of Sec. IIIC, while solid curves are results from the simpler model of Sec. IIID.